

# Confinement in a correlated Instanton-Dyon Ensemble

Miguel Angel Lopez-Ruiz<sup>1</sup>, Yin Jiang<sup>1,2</sup>, Jinfeng Liao<sup>1</sup>

<sup>1</sup>Physics Department and Center for Exploration of Energy and Matter, Indiana University, 2401 N Milo B. Sampson Lane, Bloomington, IN 47408, USA

<sup>2</sup>Institut fuer Theoretische Physik, Philosophenweg 16, D-69120 Heidelberg, Germany

E-mail: malopezr@indiana.edu

**Abstract.** Confinement is a remarkable nonperturbative phenomena emerging from QCD and QCD-like theories. A theoretical understanding of these transitions and their interrelations is of fundamental importance. While it is widely perceived that their dynamics arises from nontrivial topological configurations in Yang-Mills theories, a concrete and sophisticated realization of such idea is an outstanding challenge. We report significant progress along this direction by the construction of a new framework based on correlated ensemble of instanton-dyons, namely the constituents of the finite-temperature instantons with non-trivial holonomy. We present a comprehensive numerical study of confinement properties in SU(2) Yang-Mills theory at finite temperature, obtaining important observables such as the effective holonomy potential, the static quark potentials from Polyakov loop correlators as well as spatial Wilson loops, among others.

## 1. Introduction

The Quantum Chromodynamics, or QCD, is established as the fundamental quantum field theory of strong nuclear force underlying all of nuclear physics. Despite its great success in describing an impressive variety of nuclear phenomena in Nature, a key aspect of QCD remains mysterious and poses a great challenge to our understanding. While the theory has quarks and gluons as its basic degrees of freedom in the Lagrangian, the colored quarks and gluons are absent from the observed physical spectrum in which the various color-singlet hadronic states emerge instead. This phenomenon, often referred to with the broad term “confinement”, occurs also in a wide variety of QCD-like theories and notably in pure Yang-Mills theories. The latter fact makes it obvious that confinement arises from the nonperturbative gauge dynamics in the gluonic sector.

At finite temperature, the expectation value of the Polyakov loop at spatial infinity (holonomy)

$$L_\infty \equiv \lim_{|\vec{x}| \rightarrow \infty} \frac{1}{N_c} \text{Tr} \mathcal{P} \exp \left( i \int_0^{1/T} d\tau A_4 \right) \quad (1)$$

plays the role of the order parameter in the deconfinement phase transition; suggesting that topological gauge configurations with non-trivial holonomy may drive the mechanism of confinement.



Based on the *caloron solutions with nontrivial holonomy and nontrivial topology* to the classical Yang-Mills equations, known as the KvBLL calorons [1, 2, 3]; in particular, its “constituent” dyon fields (also called *instanton-dyons*), a promising approach has emerged for understanding the nonperturbative phenomenon of confinement through a statistical ensemble of such objects.

This talk is based on the extensive work presented in [4] where we report a thorough numerical investigation of the confinement dynamics in SU(2) Yang-Mills theory by constructing a statistical ensemble of correlated instanton-dyons. Here, we summarize our high precision results for the holonomy potential, the order parameter for confinement transition, as well as the temporal and spatial Wilson loops with an emphasis on the influence of finite volume effects.

## 2. Construction of Correlated Instanton-Dyon Ensemble

### 2.1. The Partition Function

The partition function of the instanton-dyon/antidyon ensemble is constructed from the one-loop quantum weight of the KvBLL caloron in the limit of large dyon separation [5], then extended to arbitrary number dyons and antidyons, resulting in

$$\begin{aligned} \mathcal{Z} = e^{-VP(\nu)} & \sum_{\substack{N_M, N_L, \\ N_{\bar{L}}, N_{\bar{M}}}} \frac{1}{N_L! N_M! N_{\bar{L}}! N_{\bar{M}}!} \int \prod_{l=1}^{N_L} f_L T^3 d^3 r_{L_l} \prod_{m=1}^{N_M} f_M T^3 d^3 r_{M_m} \\ & \times \prod_{\bar{l}=1}^{N_{\bar{L}}} f_{\bar{L}} T^3 d^3 r_{\bar{L}_{\bar{l}}} \prod_{\bar{m}=1}^{N_{\bar{M}}} f_{\bar{M}} T^3 d^3 r_{\bar{M}_{\bar{m}}} \det(G_D) \det(G_{\bar{D}}) e^{-V_{D\bar{D}}}, \end{aligned} \quad (2)$$

where  $f_M = \Gamma S^2 e^{-\nu S} \nu^{\frac{8\nu}{3}-1}$  and  $f_L = \Gamma S^2 e^{-\bar{\nu} S} \bar{\nu}^{\frac{8\bar{\nu}}{3}-1}$  are the fugacities per (anti)dyon species  $L, M, \bar{L}, \bar{M}$ , and the holonomy parameter  $\nu$  ( $\bar{\nu} = 1 - \nu$ ) is defined through  $L_\infty = \cos(\pi\nu)$ . The sum runs over the total number of dyons and antidyons in the system and the measure is given by the product of an uncorrelated part  $\det(G_D) \det(G_{\bar{D}})$ , namely the corresponding “*Diakonov determinants*” [6], and a correlated factor  $e^{-V_{D\bar{D}}}$  which introduces dyon-antidyon interactions given by [7][8]

$$V_{D\bar{D}} = \begin{cases} \sum_{j > \bar{j}} 2S \left( \frac{1}{\zeta_j} - 1.632 e^{-0.704\zeta_j} \right) e^{-M_D r_{j\bar{j}}} & \text{if } \zeta_j > \zeta_j^0, \text{ for } L\bar{L}, M\bar{M} \\ \sum_{i > \bar{j}} V_{ij}^C & \text{if } \zeta_j < \zeta_j^0, \text{ for } LL, \bar{L}\bar{L}, MM, \\ & \bar{M}\bar{M}, L\bar{L}, M\bar{M} \\ \sum_{i, \bar{j}} \frac{S}{\pi T r_{i\bar{j}}} e^{-M_D r_{i\bar{j}}} & \text{for } \bar{M}L, \bar{L}M \\ 0 & \text{for } LM, \bar{L}\bar{M}, \end{cases} \quad (3)$$

where  $\zeta_j = 2\pi\nu_j T r_{j\bar{j}}$ ,  $M_D$  is a screening mass introduced as a parameter,  $V_{j\bar{j}}^C = \frac{\nu_j V_c}{1 + e^{(\zeta_j - \zeta_j^0)}}$  is a repulsive core potential where  $V_c$  and  $\zeta_j^0$  are also parameters which need to be tuned for the simulations.

For simplicity, all quantities are rescaled with temperature  $T$ ; however, the temperature dependence is defined through the running of the coupling constant in the caloron action  $S$ , which at first loop approximation, is given by

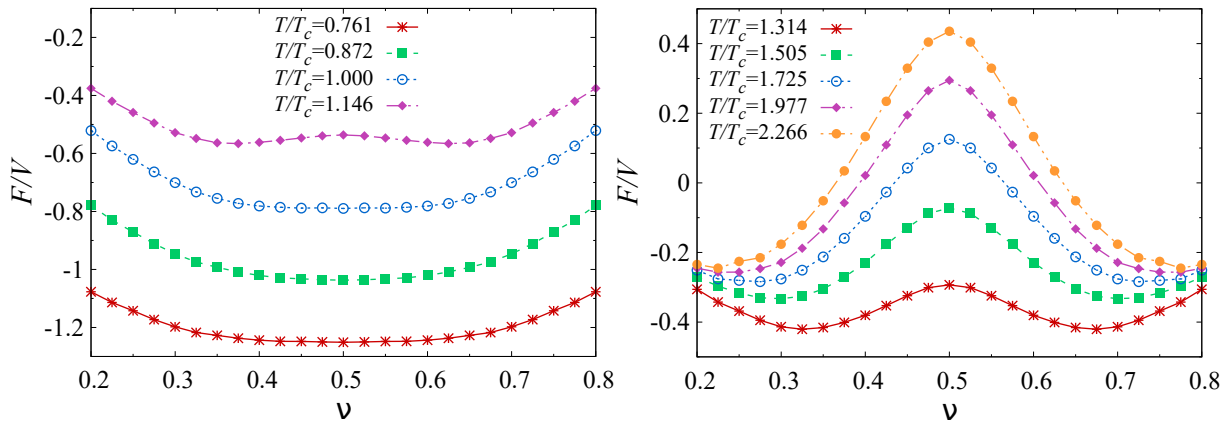


**Figure 1.** Free energy density  $F = -\log \mathcal{Z}$  of the dyon ensemble in the density range  $0 \leq n_D \leq 0.5$ .

$$S(T) = \frac{8\pi^2}{g^2(T)} = \frac{22}{3} \log \left( \frac{T}{\Lambda} \right), \quad (4)$$

where  $\Lambda$  is the scale parameter in the regularization. Therefore, by varying  $S$  as a parameter in the simulation, one can define  $\Lambda$  at the observed critical point ( $T = T_c$ ) and then establish the temperature dependence of the observables as  $T/T_c$ .

Through Monte Carlo methods, the ensemble is simulated on a box with periodic boundary conditions of volume  $V_0 = 43.37$  and a total number of (anti)dyons of each kind running from  $N_D = 0$  to 22, i.e. the dyon density range spanned was  $n_D = 0$  to 0.5.

### 3. Confinement-Deconfinement Transition

#### 3.1. The Holonomy Potential

Above some critical temperature  $T_c$ ,  $SU(2)$  pure gauge theory is expected to have a second order deconfinement phase transition, with  $\langle L_\infty \rangle$  as the order parameter characterizing its criticality. When the gauge field is that of the KvBLL caloron, the order parameter takes the form  $\langle L_\infty \rangle = \cos(\pi\nu)$ , so one expects to observe the breaking of the  $Z_2$  symmetry of the theory through the free energy density, either as a function of  $L_\infty$  or  $\nu$ .

1 shows the free energy density for  $S = 5, 6, \dots, 13$ . It was found that for  $5 \leq S \leq 7$  the minimum of the free energy density lies at  $\nu_{\min} = 0.5$ , namely maximal non-trivial holonomy. For  $S > 7$  the shape of  $F/V$  becomes that of a symmetric double well potential with  $\nu_{\min} < 0.5$ . Therefore, the critical temperature is defined at  $S = 7$ , fixing the scale parameter at  $\Lambda = 0.385T_c$ .

Universality and the Svetitsky-Yaffe conjecture [9], allow to explore the role of  $\langle L_\infty \rangle$  as an order parameter of the deconfinement phase transition, given that it should follow the power law

$$\langle L_\infty \rangle = a(T/T_c - 1)^\beta [1 + b(T/T_c - 1)^\omega], \quad (5)$$

for temperatures close to  $T_c$ . 2 shows a fit from the numerical results of the dyon ensemble in the interval  $1 \leq T/T_c \leq 1.505$ . This result shows the continuous nature of the phase transition and is in qualitative agreement with the lattice results from [10].

As for the expectation value of dyon densities, depicted in 3, one can see that at  $T \leq T_c$ , the  $L$  and  $M$  type densities are fairly equal. In the confined phase, the preferred holonomy

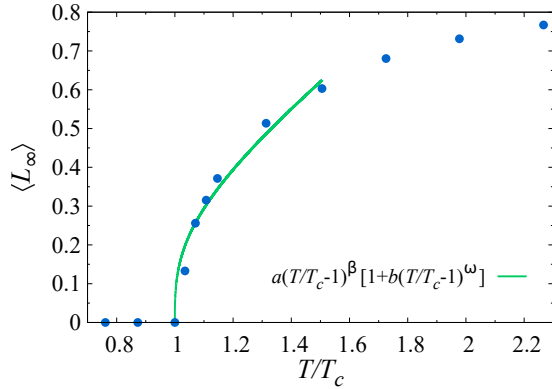


**Figure 2.**  $L_\infty$  as an order parameter of the phase transition. Fitted to the critical exponents  $\beta$  and  $\omega$  of the 3D Ising model.

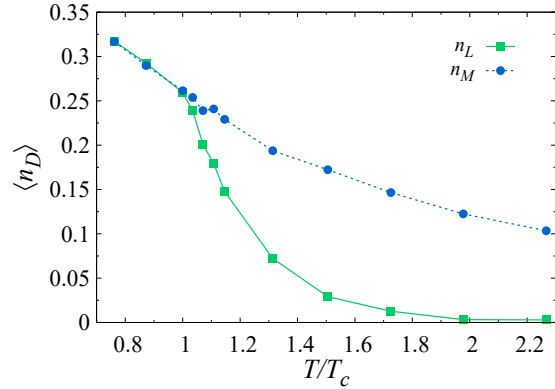


**Figure 3.** Temperature dependence of the ensemble average of dyon densities.

corresponds to the maximal non-trivial one where both dyon types have the same core radius and therefore equal weight in the partition function. For  $T > T_c$ , the preferred holonomy starts to shift towards the trivial one ( $\nu \rightarrow 0$ ) and the  $M$  dyons become larger and larger.

### 3.2. The Polyakov Loop Correlator and the Spatial Wilson Loop

In the study of confinement, it is of most importance to look at the interaction between a static (infinitely heavy) quark-antiquark pair. A successful confining theory should have an asymptotically linear rising potential at large separations between the static sources in the form  $F_{q\bar{q}}|_{|\vec{x}-\vec{y}|\rightarrow\infty} \approx \sigma_e |\vec{x}-\vec{y}|$ , where  $\sigma_e$  is the so called *electric string tension*. At finite temperature, the color averaged heavy quark-antiquark potential  $F_{q\bar{q}}^{\text{avg}}$  is defined through the expectation value of traced Polyakov loop correlators. Moreover, according to the color decomposition  $2 \otimes \bar{2} = 1 \oplus \bar{3}$ , an  $SU(2)$  quark-antiquark pair can interact through a singlet and a triplet channel like

$$e^{F_{q\bar{q}}^{\text{avg}}} = \frac{1}{4} e^{-F_{q\bar{q}}^1} + \frac{3}{4} e^{-F_{q\bar{q}}^3}, \quad (6)$$

where

$$e^{-F_{q\bar{q}}^{\text{avg}}} \equiv \frac{1}{4} \left\langle \text{Tr} L^\dagger(\vec{x}) \text{Tr} L(\vec{y}) \right\rangle \quad \text{and} \quad e^{-F_{q\bar{q}}^1} \equiv \frac{1}{2} \left\langle \text{Tr} \left[ L^\dagger(\vec{x}) L(\vec{y}) \right] \right\rangle. \quad (7)$$

On 4 we show the singlet channel free energy  $F_{q\bar{q}}^1$  as a function of interquark separation  $|\vec{x}-\vec{y}|$  for different temperatures. One can see, that below  $T_c$ , there is a linear rising potential with almost constant slope  $\sigma_e$ ; however, for  $T > T_c$ , the slope starts to decrease until it reaches values close to zero, implying a deconfined phase.

As for the spatial Wilson loop, it is known that at finite temperature it does not provide a good measure of the deconfinement phase transition, given that even above  $T_c$  it shows area law behavior and an increase of the *magnetic string tension*  $\sigma_m$  [11, 12, 13, 14]; nonetheless, the restoration of Lorentz symmetry (Euclidean  $O(4)$ ) at  $T \rightarrow 0$  suggests that in this limit,  $\sigma_m$  should coincide with the electric string tension  $\sigma_e$ . Therefore, the interest is to show that the spatial Wilson loop defined as

$$W_C \equiv \frac{1}{2} \text{Tr} \mathcal{P} \exp \left[ i \oint_C dx_i A_i(x) \right], \quad (8)$$

follows the area law

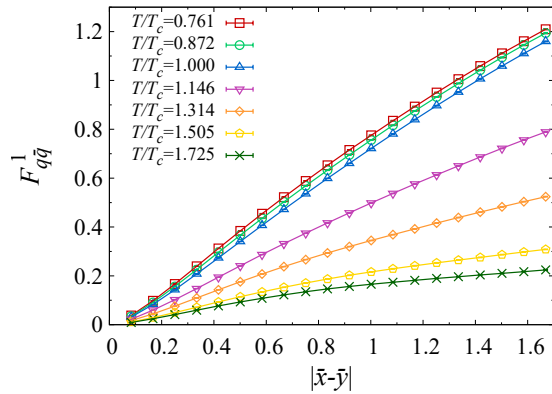


**Figure 4.** Singlet channel of the static quark-antiquark potential in the fundamental representation at confined and deconfined phases for  $\nu = 0.5, 0.5, 0.35$  and  $0.275$ , in order of increasing temperature.

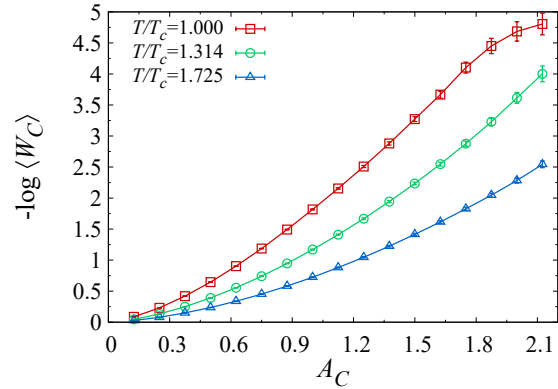


**Figure 5.** Area law for the spatial Wilson loop in the fundamental representation at confined and deconfined phases.

$$\langle W_C \rangle \sim e^{-\sigma_m A_C} \quad (9)$$

in both confining and deconfined phases. On 5, the negative logarithm of  $\langle W_C \rangle$  in the fundamental representation is plotted as a function of  $A_C$  and it can be seen that for large contour areas, indeed has an almost linear rising.

To end this section, we recall that in the units used in this work, the string tension is dimensionless, meaning that when restoring physical units it goes as  $\sigma_m \rightarrow \sigma_m/T^2$ . As has been established before,  $\sigma_m$  increases with  $T$ ; however,  $\sigma_m/T^2$  should decrease as the temperature rises [13], which is in fact in agreement with our results.

#### 4. Finite volume effects

To look into the possible effects which a finite volume have on the computed observables, we performed tests increasing the volume of the box to two and three times the previous volume used  $V_0$ .

1 contains numerical values of ensemble averages of the dyon densities at different temperatures as well as the free energy density for  $\nu_{\min}$  obtained at  $V_0$ . It can be seen that the volume effects in the densities are significantly smaller than in the free energy density, which in fact are considerably small.

Another test on the influence of volume was done with the static quark-antiquark potentials. On 6 we show the results of the singlet channel potential calculated in a box twice the size of the previous volume used. The curved tails which were present at large distances, seemed to appear only at the edge of the box, suggesting it is merely a finite volume effect of the simulation. At intermediate distances both potentials match substantially well showing the expected linear rising behavior.

#### 5. Conclusion

Confinement is a remarkable nonperturbative phenomenon in pure Yang-Mills and QCD-like theories. The mechanism of confinement remains a significant challenge to our understanding and is generally believed to pertain to certain nontrivial topological configurations of the gluonic

**Table 1.** Volume dependence of the free energy density and ensemble averages of dyon densities for  $V = V_0, 2V_0$  and  $3V_0$ , with  $V_0 = 43.37$ .

	$T/T_c$	$V_0$	$2V_0$	$3V_0$
$F/V$	0.761	-1.251	-1.275	-1.283
	1.000	-0.790	-0.813	-0.826
	1.314	-0.416	-0.433	-0.444
$\langle n_L \rangle$	0.761	0.317	0.320	0.315
	1.000	0.259	0.259	0.260
	1.314	0.075	0.077	0.077
$\langle n_M \rangle$	0.761	0.317	0.315	0.312
	1.000	0.261	0.262	0.259
	1.314	0.215	0.216	0.215

sector. The recently found KvBLL caloron solutions with nontrivial holonomy, consisting of constituent dyons, have provided a concrete and promising path of investigation. We conclude that an ensemble of such objects correctly produces the various essential features of the confinement dynamics from above to below the transition temperature. These features include the evolution of holonomy potential with temperature, a second order phase transition in terms of the order parameter (Polyakov loop expectation value), the linear static quark-anti-quark potential, etc. Given such success, it appears reasonable to believe that the ensemble of correlated instanton-dyons may indeed hold the key of confinement mechanism.

### Acknowledgements

The authors are particularly grateful to E. Shuryak for many helpful discussions. The authors also thank R. Larsen, E.-M. Ilgenfritz, M. Faber, R. Pisarski, I. Zahed, and A. Zhitnitsky for useful discussions and communications. This work is supported by the National Science Foundation under Grant No. PHY-1352368. MALR is in addition supported by CONACyT under Doctoral supports Grants No. 669645. The computation of this research was performed on IU's Big Red II cluster that is supported in part by Lilly Endowment, Inc. (through its

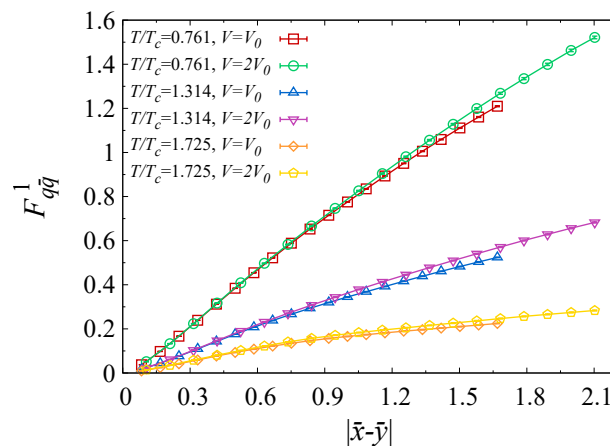


**Figure 6.** Volume effects on the singlet channel of the static quark-antiquark potential at confined and deconfined phases.

support for the Indiana University Pervasive Technology Institute) and in part by the Indiana METACyt Initiative.

## References

- [1] T. C. Kraan and P. van Baal, *Nucl. Phys. B* **533**, 627 (1998) [hep-th/9805168].
- [2] T. C. Kraan and P. van Baal, *Phys. Lett. B* **435**, 389 (1998) [hep-th/9806034].
- [3] K. M. Lee and C. h. Lu, *Phys. Rev. D* **58**, 025011 (1998) [hep-th/9802108].
- [4] M. A. Lopez-Ruiz, Y. Jiang and J. Liao, *Preprint* arXiv:1611.02539 [hep-ph].
- [5] D. Diakonov, N. Gromov, V. Petrov and S. Slizovskiy, *Phys. Rev. D* **70**, 036003 (2004) [arXiv:hep-th/0404042].
- [6] D. Diakonov and V. Petrov, *Phys. Rev. D* **76**, 056001 (2007) [arXiv:0704.3181 [hep-th]].
- [7] R. Larsen and E. Shuryak, *Nucl. Phys. A* **950**, 110 (2016) [arXiv:1408.6563 [hep-ph]].
- [8] R. Larsen and E. Shuryak, *Phys. Rev. D* **92**, no. 9, 094022 (2015) [arXiv:1504.03341 [hep-ph]].
- [9] B. Svetitsky and L. G. Yaffe, *Nucl. Phys. B* **210**, 423 (1982).
- [10] S. Digal, S. Fortunato and P. Petreczky, *Phys. Rev. D* **68**, 034008 (2003) [hep-lat/0304017].
- [11] C. Borgs, *Nucl. Phys. B* **261**, 455 (1985).
- [12] E. Manoussakis and J. Polonyi, *Phys. Rev. Lett.* **58**, 847 (1987).
- [13] G. S. Bali, J. Fingberg, U. M. Heller, F. Karsch and K. Schilling, *Phys. Rev. Lett.* **71**, 3059 (1993) [hep-lat/9306024].
- [14] L. Karkkainen, P. Lacock, D. E. Miller, B. Petersson and T. Reisz, *Phys. Lett. B* **312**, 173 (1993) [hep-lat/9306015].